Edge effects on the characteristics of uranium diffusion on graphene and graphene nanoribbons*

Cheng Cheng(程诚)[1,†], Han Han(韩晗)[1], Cui-Lan Ren(任翠兰)[1,2], Chang-Ying Wang(王昌英)[1,3], Kuan Shao(邵宽)[1], and Ping Huai(怀平)[1,‡]

[1] *Shanghai Institute of Applied Physics, Chinese Academy of Sciences, Shanghai* 201800, *China*
[2] *Key Laboratory of Interfacial Physics and Technology, Chinese Academy of Sciences, Shanghai* 201800, *China*
[3] *University of Chinese Academy of Sciences, Beijing* 100049, *China*

(Received 19 January 2016; revised manuscript received 7 April 2016; published online 25 June 2016)

The first principles density-functional theoretical calculations of U adatom adsorption and diffusion on a planar graphene and quasi-one-dimensional graphene nanoribbons (GNRs) are performed. An energetic preference is found for U adatom diffusing to the hollow sites of both graphene and GNRs surface. A number of U distinctive diffusion paths either perpendicular or parallel to the ribbon growth direction are examined. The edge effects are evidenced by the calculated energy barriers of U adatom diffusion on armchair and zigzag nanoribbons surfaces. The calculation results indicate that the diffusion of U adatom from the inner site toward the edge site is a feasible process, particularly in zigzag GNR. It is viable to control the initial morphology of nuclear carbon material to retard the diffusion and concentration of nuclides.

Keywords: diffusion, armchair GNR, zigzagGNR, edge effects

PACS: 63.20.dk, 42.25.Gy, 68.49.Bc **DOI:** 10.1088/1674-1056/25/8/086301

1. Introduction

Since its first discovery in experiment in 2004,[1] graphene has aroused rapidly increasing research interest in both low-dimensional physical research and applications such as biological engineering, optical electronics, ultrafiltration, photovoltaic cells, energy storage and composite materials.[2] Particularly, composite materials have been considered as the most promising candidates for Generation IV nuclear reactor structural materials and nuclear fuel materials. For instance, actinide fuels and fission products are enclosed into the pyrocarbon buffer layer and silicon carbide layers of the TRISO coated fuel particles, which are all sealed with a graphite shell.[3] The radioactive nuclides will leak into the primary circuit through both pristine and defective structures, such as morphologies of vacancies, voids and cracks. It is important to investigate the behaviors of nuclides on the monolayer graphene that is patterned with pores, gaps or fabricated into ribbons, whose edge configurations are important for properties.[4,5]

In experimental studies, a system of small metal adatoms on graphene can be created with transmission electron microscopy (TEM).[6–10] The structural characterization can be performed with high-resolution low-energy electron diffraction (LEED) and high-resolution electron energy-loss spectroscopy (EELS) to investigate the properties of adsorption and diffusion by measuring the excitation spectra.[11–14] Many efforts have been devoted to investigate the existence of metal-graphene structures. So far, most of these researches mainly focused on transition metal atoms[4–8] to open the unique zero band gap, and lithium atom for energy storage application.[15] There are limited investigations about metal atoms diffusion on strained graphene,[16] particularly for nuclide atoms and fission product metal atoms.[11,17] Londono *et al.* have reviewed the progress in the field of fission product sorption in carbon structures.[18]

In the respect of theoretical simulations, metal atom adsorption and diffusion on both graphene and graphene nanoribbons (GNRs) have been investigated extensively. For the metal elements from groups I to III of the periodic table, the results are consistent with ionic bonding.[19–23] For transition metals (TMs), the results are consistent with covalent bonding, and adsorption is characterized by strong hybridization between adatoms and graphene electronic states.[24–30] The hollow site is found to be the more stable one for 3d TM.[24,25] However, noble metals prefer the top site rather than the hollow site of graphene due to weak bonding interaction.[19,20] The adsorption and desorption of four kinds of main radioactive productions (Cs, U, Sr, Ag) on the graphite surface have also been studied.[31] Besides, there are plenty of studies for non-metallic atoms,[30,32] metal lithium atom,[33–35] and TM atoms diffusion on GNRs.[26–29] Both

*Project supported by the International S & T Cooperation Program of China (Grant No. 2014DFG60230), the National Natural Science Foundation of China (Grant Nos. 91326105, 21306220, and 21501189), and the Strategic Priority Research Program of the Chinese Academy of Sciences (Grant No. XDA02040104).

†Corresponding author. E-mail: chengcheng@sinap.ac.cn
‡Corresponding author. E-mail: huaiping@sinap.ac.cn

© 2016 Chinese Physical Society and IOP Publishing Ltd

experimental investigations and theoretical calculations have shown that the edges and geometries of graphene sheets can have a fundamental influence on their electronic properties.

With the development of carbon nano-materials in the nuclear material field, it is inevitable for both scientific and technological research to investigate the interaction between nucleus and carbon material, which is of great importance for nuclear reactor safety.[36] Burns has reviewed the current understanding of nuclear fuel interaction with the environment, including nanoscale actinide materials promoting the dissolution of fuel.[37] Shi *et al.* have reviewed the current basic research progress of nano-materials and nano-technologies in advanced nuclear fuel fabrication, spent nuclear fuel reprocessing, nuclear waste disposal and nuclear environmental restoration.[5] There are several interesting studies about metallofullerene containing actinide metal atoms or molecules with both experimental studies[38–41] and theoretical simulations for unique properties of actinide metal bonding.[42–46] Furthermore, there are several studies about actinide molecule adsorption and vibrations on graphene derivatives: pristine single and double layer graphene, as well as hydrogenated and fluorinated graphene,[47,48] and actinide ions adsorption on graphene oxides.[49–51] However, to date, no conclusive experimental data or theoretical simulation results have been obtained for the adsorption and diffusion of nuclides on GNRs surface.

With regard to the interactions between actinide materials and coated carbon nano-materials of nuclear fuel, a simple theoretical model has been adopted for studying actinide adatom adsorption and diffusion on graphene and GNRs. In the present work, we perform the first principles calculations within density-functional theory (DFT). The adsorption energies of U adatom on graphene and GNRs are benchmarked within both the local density approximation (LDA) and PBE results. A number of U diffusion paths either perpendicular or parallel to the ribbon growth direction are taken into consideration. Owing to the one-dimensional (1D) structure, the characteristics of U atom diffusion would be strongly dependent on the specific morphology of the edges. The edge effect can be elucidated with energy barriers of the U atom diffusion on both armchair and zigzag graphene nanoribbons (armchair-GNRs and zigzag-GNRs) compared with the graphene surface.

2. Method and calculations

Using the "Vienna *ab initio* simulation package" (VASP) code,[52–54] we perform the first principle calculations within the density-functional theory (DFT)[55] about U adatom adsorption and diffusion on graphene and quasi-one-dimensional graphene nanoribbons with well-defined edge morphologies. In this section, we describe the calculation model and parameters used in the calculations.

The electron-ion interaction is modeled by using the projector-augmented wave (PAW) method.[56] The exchange–correlation is identified within the LDA[57] and the generalized gradient approximation (GGA) of Perdew, Burke and Ernzernhof (PBE).[58,59] Although the U-graphene interaction is well described by either LDA or GGA functional, the GGA results are used because of its ability to describe the large variation of electron density.[60] In Section 3, the energies are compared with the LDA and PBE results of U adsorption on hollow, top, and bridge sites of graphene, and some particular sites on armchair-GNRs and zigzag-GNRs.

The plane-wave basis set with a 500-eV cutoff energy is used. The Brillouin zone integration is performed on a special k-point sampling according to the Monkhorst–Pack scheme[61] with a Γ-centered grid. For adsorption energy calculations, the k point is adopted as 7×7 grid for graphene, and 7 uniform grid for 1D nanoribbon. In geometry optimization, the atoms are allowed to relax until the force on the atom is less than 0.01 eV/Å and the energy on the atom is less than 10^{-5} eV.

In this work, we chose three typical systems of graphite material surfaces. The unit of a single layer graphitic surface is an isolated 4×4 supercell of a two-dimensional (2D) graphene (without replica in the z direction) with 32 C atoms and 1 U atom. It has been recognized that the morphology of the graphitic edge can affect the behaviour of an adatom. Thus, we choose an isolated supercell of 1.72-nm wide armchair graphene nanoribbons (armchair-GNRs) containing 60C atoms, 8 H atoms passivating the edges and 1 U atom, and 1.57-nm wide zigzag graphene nanoribbons (zigzag-GNRs) containing 64 C atoms, 8 H atoms passivating the edges and 1 U atom. The three systems all have a 15-Å vacuum spacing between the layers to prevent interaction between repeated images.

According to the energy barriers of different paths, we can study the characteristics of U atom diffusing on graphene and GNRs. While these energies are calculated as the difference in adsorption energy between the stable states and the saddle points along the diffusion paths. The theoretical results are equal to the nudged elastic band (NEB)[62–64] results. We calculate the adsorption energy which is defined as follows:

$$E_{\mathrm{ad}} = -E_{\mathrm{Total}} - E_{\mathrm{Graphene}} - E_{\mathrm{U-atom}},$$

where E_{ad} is the adsorption energy; E_{Graphene} is the energy of graphene (or GNR); $E_{\mathrm{U-atom}}$ is the energy of an isolated U atom; E_{Total} is the total energy of adatom-graphene (or GNR) systems.

3. Results and discussion

3.1. Adatom adsorption on graphene and graphene nanoribbons

We first calculate the energy of a single U adatom adsorption on graphene surface. Owing to the high-symmetry hexagonal structure of graphene, the adsorbed sites are usually classified as three types: top (T), bridge (B), and hollow (H) sites as shown in Fig. 1. For the top site adsorption, the U atom is located directly above one carbon atom of graphene. For the bridge site adsorption, the U atom is located above the middle of the C–C bond. For the hollow site adsorption, the U atom is located above the centre of a hexagon structure. The lattice constants are fixed through optimization, and the coordinates of all the carbon atoms and adatoms are allowed to be relaxed. In this work, we study the interaction between U adatom with the graphite material surface, and verify that the hollow sites are the most stable in the cases of both graphene and graphene nanoribbons. The adsorption energies of the adatom in three sites are given in Table 1. The most stable position for the U adatom is the hollow site of a hexagon of bond, with adsorption energies being −2.61 eV for LDA and −1.97 eV for PBE respectively. The lowest energy site is found to be the top site, with adsorption energies being −2.28 eV for LDA and −1.58 eV for PBE respectively. Although the hollow adsorption site is most stable for the U atom, the distortion of graphene (Δh) is the smallest indicated by both LDA and PBE calculations, which is less than 0.1 Å. The graphene surface is weakly perturbed by the U adatom at the hollow site. However, the U adatoms on the top site and bridge site cause much larger distortion for the graphene surface. Based on previous work on main fission production atom adsorption on graphite surface, the hollow site is more stable for Cs and Sr adsorption on graphene, with adsorption energies being −0.54 eV and −0.53 eV in the generalized gradient approximation, respectively. The energies increase to −2.20 eV and −2.70 eV of adatom on the defective monolayer graphite.[31] The present results indicate that the U atoms are more easily trapped by the pristine graphene hollow sites, while fission production atoms are trapped by vacancies on the graphene surface.

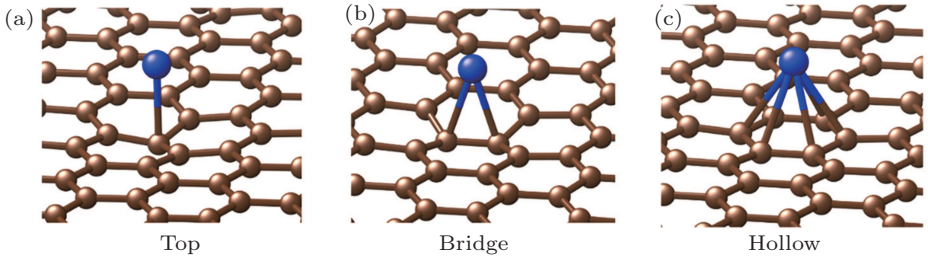


Fig. 1. (color online) Optimized structures of U adsorbed on graphene: (a) top site, (b) bridge site, (c) hollow site. The brown atoms denote carbon atoms in the super cell and the blue atoms represent the U atom.

Table 1. Calculated values of adsorption energy (E_{ad}), adsorption height of U atom (h), the distance between the U atom and the nearest C atom (d), and graphene distortion (Δh). Schematic diagram of h, d, and Δh are shown in Fig. 2.

	E_{ad}/eV	h/Å	d/Å	Δh/Å
T-site/LDA	–2.28	1.97	2.36	0.38
B-site/LDA	–2.34	1.92	2.40	0.37
H-site/LDA	–2.61	2.03	2.56	0.09
T-site/PBE	–1.58	2.17	2.43	0.26
B-site/PBE	–1.60	2.14	2.47	0.22
H-site/PBE	–1.97	2.16	2.64	0.05

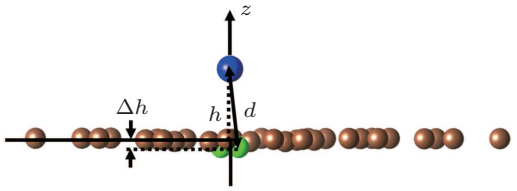


Fig. 2. (color online) Optimized structure of U adsorbed on the bridge site of graphene in side view. The brown atoms denote the carbon atoms in the supercell, the blue atom represents the U atom, and the green atoms refers to the nearest carbon atoms to the U atom. Symbol 'h' in the dot line denotes the adsorption height of the U atom; symbol 'd' in the solid line represents the distance between the U atom and the nearest C atom; and symbol 'Δh' between the two arrows refers to the graphene distortion.

Furthermore, we investigate whether the energy barrier is sensitive to the choice of the functional. The adsorption energies of the U atom on the armchair and zigzag nanoribbons, from the LDA and PBE calculations are shown in Fig. 3. As is well known, the LDA tends to overestimate the adsorption energy, and the PBE results usually tend to underestimate for the systems in which the van der Waals interaction is important.[65] Thus, the real adsorption energies are expected to be a moderate value between LDA and PBE results. In the previous studies, PBE calculations are generally used in the systems of GNRs interaction with copper-family-element atoms,[66] and transition metal atoms.[26,27]

In comparison to the most stable hollow sites in the systems shown in Fig. 3, the adsorption energies in the zigzag-GNRs system are larger than those in the armchair-GNRs system within both LDA and PBE functionals. It is obvious that the interaction of the U atom with zigzag-GNRs is much stronger than that with armchair-GNRs. The benchmark of two fully relaxed approaches with LDA and PBE shows that there is no significant effect when obtaining the adsorption energies of the present systems except for a certain different

value. In order to obtain the diffusion tendency results at the same level of calculation, we use the PBE approximation for each U atom diffusion position for the following studies of graphene nanoribbons.

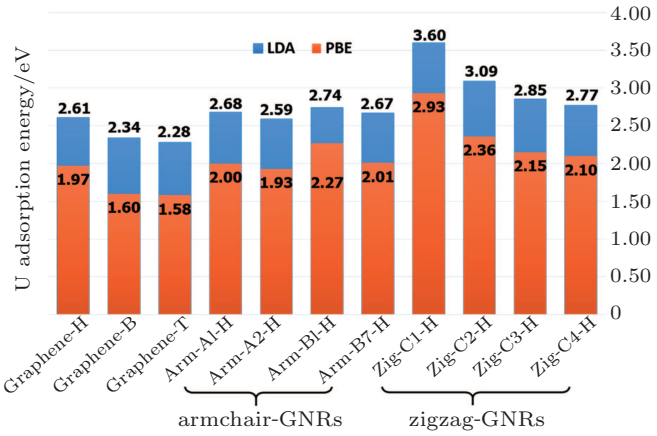


Fig. 3. (color online) Absolute values of U atom adsorption energies on the hollow sites of the different systems considered by LDA and PBE: (4×4) graphene super cell, the hollow sites of diffusing paths on armchair-GNRs and zigzag-GNRs (shown in Figs. 5, 7, and 9). For instance, Arm-A1-H denotes the binding energy of the starting hollow site of diffusion path A1 in armchair-GNRs system.

3.2. Migration on armchair and zigzag graphene nanoribbons

In order to analyse the characteristics of U atoms diffusing on the surfaces of graphene and GNRs, we calculate the energy differences of the stable states and the saddle points along several typical diffusion paths. With the U atom shifting from the centre to the edge of GNRs, the interaction between atom and nanoribbons surface displays the strong edge effect of zigzag-GNRs. For the edge effect, the adsorbate atom has the same probability of migration to both edges. It shows different appearances only if the GNRs have two different edge shapes. Thus, both the width and length of GNR will only influence the number and values of energy barriers, but not the tendency of the edge effect.

It should be noted that we calculate the adsorption energies of different sites by using the rigid model approach. Thus, all the energies of U atom diffusion paths could be obtained at the same level of calculations. The diffusion tendency is elucidated more efficiently by varying the U atom distance to the carbon nanostructure surface until the most stable position is found. Even the stronger adsorption effects at the nanoribbons edges do not deform the carbon hexagonal structure. In a previous study of the characteristic of Li diffusion on graphene, the adsorption energies of Li were tested by using the rigid model approach and fully relaxed approach with LDA and PBE functional.[33] The results with two models achieve the equilibrium distance.

First, we study the diffusion behavior of the U atom on the 2D graphene surface, which is compared afterwards with its behavior on the 1D GNR surface. Owing to the symmetry of the honeycomb lattice, there are two different mechanisms for adatom diffusion on a graphene surface. As shown in Fig. 4, path A is from the hollow site of the hexagon (H) through the bridge site (B) of the bond. The U atom diffuses repeatedly through H→B→H sites. Path B is from the hollow site of the hexagon (H) through the top of a carbon atom (T) and the bridge (B) site of the bond. The U atom diffuses repeatedly through H→T→B→T→H sites. The barrier heights for these two paths are 0.45 eV and 0.46 eV respectively, by comparing with energy barriers of the various diffusion paths on GNRs.

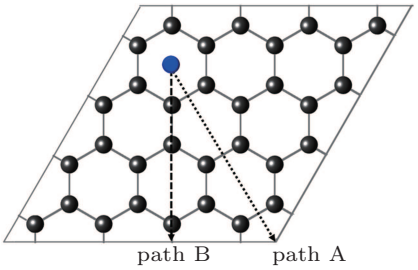


Fig. 4. (color online) Schematic representation of the graphene cell used in the calculations and two diffusion paths of A and B on graphene.

When the monolayer graphene is patterned with gaps or fabricated into ribbons, the symmetry of the honeycomb lattice is broken. GNRs are typical structures like quasi-one-dimensional slices of graphene. The hexagons from the centre of the nanoribbons toward the edge are not equivalent any more. Thus, the properties are sensitive to the edge configurations of GNRs. We first calculate the adsorption energies of U diffusion along different paths in armchair-GNRs. As shown in Figs. 5 and 6, we identify two distinctive paths A1 and A2 for U atom diffusion from the centre of the armchair-GNRs through the bridge of the bond, and to the edge in the end. The U atom diffuses repeatedly through H→B→H site, which is vertical to the periodic direction. The barrier energies of paths A1 and A2 are compared with that of the main path A in the graphene surface. We verify that the E_{ad} results of the centre of the GNRs hollow sites are almost the same as the E_{ad} results of the hollow site on the graphene surface. The energy barrier of the initial hollow site in path A1 is about 0.04 eV larger than in the graphene in the centre of the nanoribbons. When the U atom moves to the edge of armchair-GNRs, the energy barriers significantly increase 0.72 eV and 0.43 eV for paths A1 and A2, respectively. Otherwise, the energy barrier of path A1 increases to 0.91 eV for diffusion from the hollow site to the bridge site of the edge. It is obvious that the U atom is inclined to stay at the hollow site near the edge of armchair-GNRs. In the case of path B1 and B7 shown in Fig. 7, the U atom is diffusing repeatedly through H→T→B→T→H sites, of which the path is parallel to the edge of armchair-GNRs. In Fig. 8, it is clearly shown that the adsorption energies of path B7 are consistent with the diffusion tendency in graphene

surface, while the energy barrier of path B1 is about 0.66 eV larger than that of B7. The number of non-equivalent diffusion paths for type B is relevant with the width of GNRs. Owing to the U diffusion barriers of types A and B, there is no noticeable edge effect in the case of armchair-GNRs.

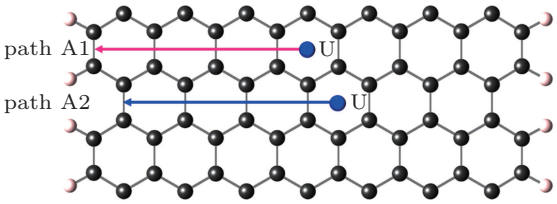


Fig. 5. (color online) Schematic representation of the armchair-GNR cell and two diffusion paths of A1 and A2.

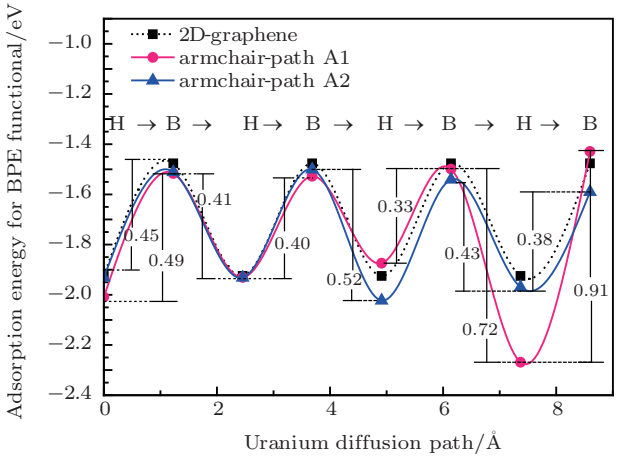


Fig. 6. (color online) Energy barriers for uranium atom diffusion path A on graphene, path A1 and path A2 on armchair-GNR.

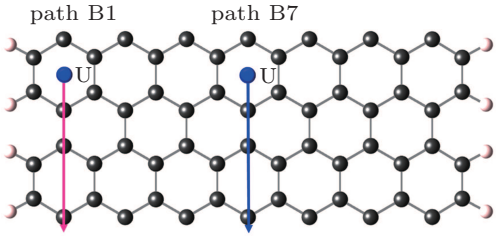


Fig. 7. (color online) Schematic representation of the armchair-GNR cell and two diffusion paths of B1 and B7.

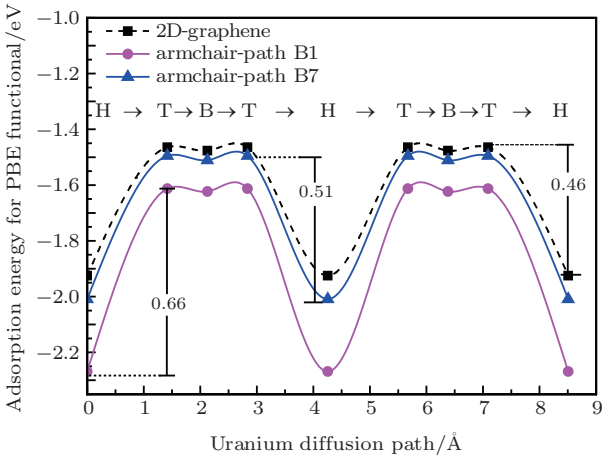


Fig. 8. (color online) Energy barriers for uranium atom diffusion path B on graphene, path B1 and path B7 on armchair-GNR.

In the case of zigzag-GNRs, it is remarkable that the edge effects are more pronounced than those in the armchair-GNRs. Like the armchair-GNRs case, diffusion paths in C type are first considered, which are parallel to the edge of nanoribbons as shown in Figs. 9 and 10. According to the ribbon width, we identify four paths that the U atom moves through H→B→H sites repeatedly along the periodic direction. The energy barrier of path C1, which is nearest to the edge of GNRs, is almost 0.36 eV, about 0.09 eV lower than in the graphene surface. The adsorption energy of the U atom at the edge of zigzag-GNR is about 50% higher than that on the graphene surface. With the adsorption site shifting from the centre to the edge of ribbons, the interaction between adatom and zigzag-GNRs becomes stronger.

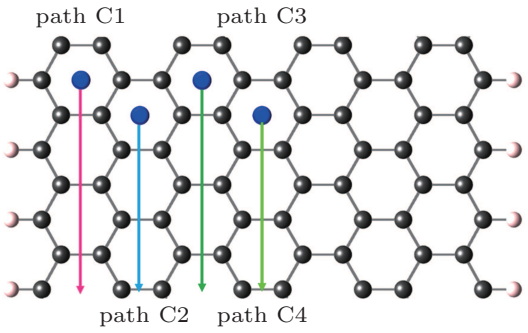


Fig. 9. (color online) Schematic representation of the zigzag-GNR cell and four diffusion paths of C1, C2, C3, and C4.

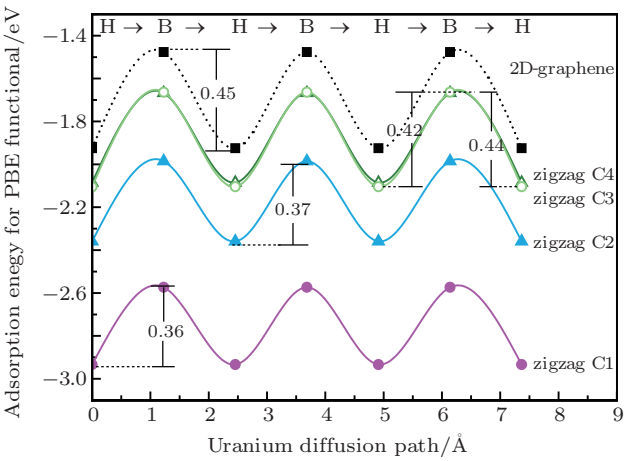


Fig. 10. (color online) Energy barriers for uranium atom diffusion path A on graphene, paths C1, C2, C3, and C4 on zigzag-GNR.

Compared with the cases in armchair-GNRs, it is easier for the U adatom to diffuse and accumulate at the edge in zigzag-GNRs. For other diffusion paths D and E as shown in Fig. 11, which are in the vertical and slant direction to the periodic direction respectively, we study the energy barriers of paths D1 and E1 as shown in Figs. 12 and 13 respectively. We can find the same tendency of U atom diffusion as that of path C type. The adsorption energies systematically decrease towards the edge. Once U atoms diffuse to the edge of zigzag-GNRs, they tend to stay and accumulate at the edge hollow sites.

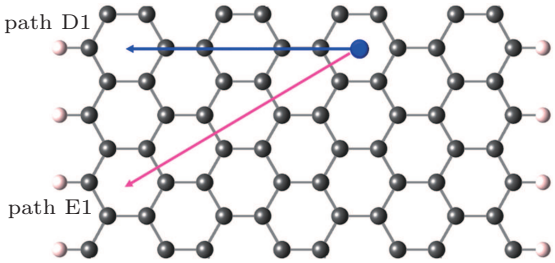


Fig. 11. (color online) Schematic representation of the zigzag-GNR cell and two diffusion paths of D1 and E1.

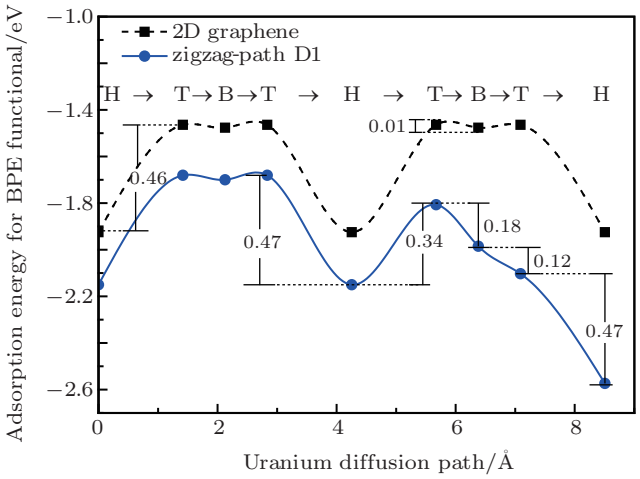


Fig. 12. (color online) Energy barriers for uranium atom diffusion path B on graphene and path D1 on zigzag-GNR.

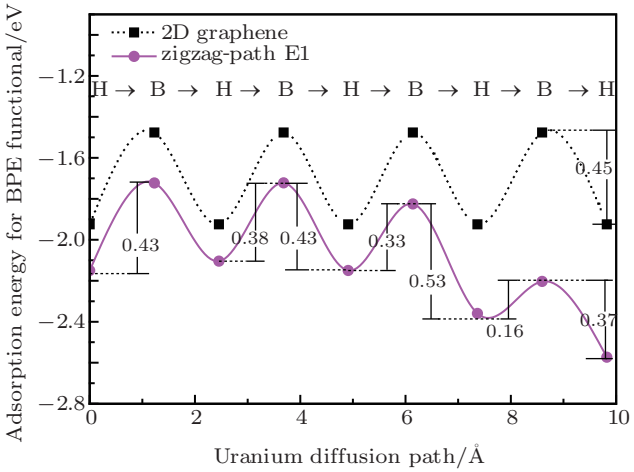


Fig. 13. (color online) Energy barriers for uranium atom diffusion path A on graphene and path E1 on zigzag-GNR.

4. Conclusions

In this work, we study the adsorption behaviours of the main nuclide U on a pristine graphene surface. Using the first-principles density-functional theory, we investigate the stable adsorption sites, the adsorption heights and distortions for U and the graphene system. The most stable position for the U adatom is at the hollow site of a hexagon of bonds, with adsorption energies of −2.61 eV for LDA and −1.97 eV for PBE respectively. However, the U adatom on the top site and bridge site causes much larger distortion of the graphene surface.

Under high temperature and high irradiation circumstances, the graphite materials will exhibit both pristine and defective structures. When the symmetry of the honeycomb lattice is broken, it is necessary to investigate the behaviours of nuclides on the monolayer graphene, whose edge configurations will strongly affect their properties. We identify several distinctive diffusion pathways of graphene surface, armchair-GNRs and zigzag-GNRs. Based on the energy barriers of U atom diffusion characteristics, the edge effects are more pronounced in zigzag-GNRs than in the armchair-GNRs. Thus, U adatoms tend to stay and accumulate at the zigzag edge in the graphene surface. These results illustrate the importance of controlling the initial morphology of nuclear graphite materials for sustainable nuclear fuel materials.

References

[1] Novoselov K S, Geim A K, Morozov S V, Jiang D, Zhang Y, Dubonos S V, Grigorieva I V and Firsov A A 2004 *Science* **306** 666
[2] Geim AK 2009 *Science* **324** 1530
[3] Verfondern K, Nabielek H and Kendail J M 2007 *Nucl. Eng. Technol.* **39** 603
[4] Yan L, Zheng Y B, Zhao F, Li S J, Gao X F, Xu B Q, Weiss P S and Zhao Y L 2012 *Chem. Soc. Rev.* **41** 97
[5] Shi W Q, Yuan L Y, Li Z J, Lan J H, Zhao Y L and Chai Z F 2012 *Radiochimca Acta* **100** 727
[6] Gan Y, Sun L and Banhart F 2008 *Small* **4** 587
[7] Zan R, Bangert U, Ramasse Q and Novoselov K S 2012 *Nano Lett.* **11** 1087
[8] Zan R, Bangert U, Ramasse Q and Novoselov K S 2011 *Small* **7** 2868
[9] Zan R, Ramasse Q, Bangert U and Novoselov K S 2012 *Nano Lett.* **12** 3936
[10] Ramasse Q, Zan R, Bangert U, Boukhvalov D W and Son Y W 2012 *ACS Nano* **6** 4063
[11] Gleeson M, Kasemo B and Chakarov D 2003 *Surf. Sci.* **524** L77
[12] Li Z Y, Hock K M and Palmer R E 1991 *Phys. Rev. Lett.* **67** 1562
[13] Li Z Y, Hock K M, Palmer R E and Annett J F 1991 *J. Phys.: Condens. Matter* **3** 103
[14] Hunt M R C, Durston P J and Palmer R E 1996 *Surf. Sci.* **364** 266
[15] Pumera M 2011 *Energy Environ. Sci.* **4** 668
[16] Cretu O, Krasheninnikov A V, Rodríguez-Manzo J A, Sun L T, Nieminen R M and Banhart F 2010 *Phys. Rev. Lett.* **105** 196102
[17] Prezzi D, Eom D, Rim K T, Zhou H, Xiao S X, Nuckolls C, Heinz T F, Flynn G W and Hybertsen M S 2014 *ACS Nano* **8** 5765
[18] Londono H A, Szlufarska I, Bratton R and Morgan D 2012 *J. Nucl. Mater.* **426** 254
[19] Chan K T, Neaton J and Cohen M L 2008 *Phys. Rev. B* **77** 235430
[20] Liu X, Wang C Z, Hupalo M, Lu W, Tringides M C, Yao Y and Ho K M 2012 *Phys. Chem. Chem. Phys.* **14** 9157
[21] Meng S and Gao S 2006 *J. Chem. Phys.* **125** 014708
[22] Meng S, Chakarov D V, Kasemo and Gao B S 2004 *J. Chem. Phys.* **121** 12572
[23] Zhou L J, Hou Z F and Wu L M 2012 *J. Phys. Chem. C* **116** 21780
[24] Valencia H, Gil A and Frapper G 2010 *J. Phys. Chem. C* **114** 14141
[25] Cao C, Wu M, Jiang J and Cheng H P 2010 *Phys. Rev. B* **81** 205424
[26] Longo R C, Carrete J and Gallego L J 2011 *Phys. Rev. B* **83** 234515
[27] Wang Z Y, Xiao J R and Li M 2013 *Appl. Phys. A* **110** 235
[28] Yu G D, Lü X L, Jiang L W, Gao W Z and Zheng Y S 2013 *J. Phys. D: Appl. Phys.* **46** 375303
[29] Sevincli H, Topsakal M, Durgun E and Ciraci S 2008 *Phys. Rev. B* **77** 195434
[30] Ataca C, Aktürk E, Sahin H and Ciraci S 2011 *J. Appl. Phys.* **109** 013704
[31] Luo X F, Fang C, Li X, Lai W S, Sun L F and Liang T X 2013 *Appl. Surf. Sci.* **285** 278
[32] Lan J, Zheng X H, Song L L, Wang R N and Zeng Z 2012 *Solid State Commun.* **152** 1635
[33] Uthaisar C, Barone V and Peralta J E 2009 *J. Appl. Phys.* **106** 113715

[34] Krepel D and Hod O 2011 *Surf. Sci.* **605** 1633
[35] Uthaisar C and Barone V 2010 *Nano Lett.* **10** 2838
[36] Nano Nuclear 2012 *Collaborative Report on the Workshop*, June 6–8, 2012, Gaithersburg, Maryland
[37] Burns P C 2012 *Science* **335** 1184
[38] Guo T, Diener M D, Chai Y, Alford M J, Haufler R E, McClure S M, Ohno T, Weaver J H, Scuseria G E and Smalley R E 1992 *Science* **257** 1661
[39] Diener M D, Smith C A and Veirs D K 1997 *Chem. Mater.* **9** 1773
[40] Sueki K, Kikuchi K, Akiyama K, Sawa T, Katada M, Ambe S, Ambe F and Nakahara H 1999 *Chem. Phys. Lett.* **300** 140
[41] Akiyama A, Zhao Y L, Sueki K, Tsukada K, Haba H, Nagame Y, Kodama T, Suzuki S, Ohtsuki T, Sakaguchi M, Kikuchi K, Katada M and Nakahara H 2001 *J. Am. Chem. Soc.* **123** 181
[42] Liu X, Li L, Liu B, Wang D Q, Zhao Y L and Gao X F 2012 *J. Phys. Chem. A* **116** 11651
[43] Gagliardi L and Roos B O 2005 *Nature* **433** 848
[44] Lu X, Feng L, Akasaka T and Nagase S 2012 *Chem. Soc. Rev.* **41** 7723
[45] Dai X, Cheng C, Zhang W, Xin M S, Huai P, Zhang R Q and Wang Z G 2013 *Sci. Rep.* **3** 1341
[46] Dai X, Xin M S, Meng Y, Han J, Gao Y, Zhang W, Jin M X, Wang Z G and Zhang R Q 2014 *Carbon* **78** 19
[47] Koh Y W, Westerman K and Manzhos S 2015 *Carbon* **81** 800
[48] Han J, Dai X, Cheng C, Xin M S, Wang Z G, Huai P and Zhang R Q 2013 *J. Phys. Chem. C* **117** 26849
[49] Wu Q Y, Lan J H, Wang C Z, Zhao Y L, Chai Z F and Shi W Q 2014 *J. Phys. Chem. A* **118** 10273
[50] Wu Q Y, Lan J H, Wang C Z, Xiao C L, Zhao Y L, Wei Y Z, Chai Z F and Shi W Q 2014 *J. Phys. Chem. A* **118** 2149
[51] Li Z J, Chen F, Yuan L Y, Zhao Y L, Chai Z F and Shi W Q 2012 *Chem. Eng. J.* **210** 539
[52] Kresse G and Hafner J 1993 *Phys. Rev. B* **47** 558
[53] Kresse G and Furthmüller J 1996 *Phys. Rev. B* **54** 11169
[54] Kresse G and Furthmüller J 1996 *Comput. Mater. Sci.* **6** 15
[55] Kohn W and Sham L 1965 *Phys. Rev. B* **140** 1133
[56] Blöchl P E 1994 *Phys. Rev. B* **50** 17953
[57] Perdew J P and Wang Y 1992 *Phys. Rev. B* **45** 13244
[58] Perdew J P, Ruzsinszky A, Csonka F I, Vydrov O A, Scuseria G E, Constantin L A, Zhou X L and Burke K 2008 *Phys. Rev. Lett.* **100** 136406
[59] Perdew P E, Burke K and Ernzerhof M 1996 *Phys. Rev. Lett.* **77** 3865
[60] S. Kurth, Perdew J P and Blaha P 1999 *Int. J. Quantum Chem.* **75** 889
[61] Monkhorst H J and Pack J D 1976 *Phys. Rev. B* **13** 5188
[62] Henkelman G, Uberuaga B P and Jónsson H 2000 *J. Chem. Phys.* **113** 9901
[63] Henkelman G and Jónsson H 2000 *J. Chem. Phys.* **113** 9978
[64] Sheppard D, Terrell R and Henkelamn G 2008 *J. Chem. Phys.* **128** 134106
[65] Vanin M, Mortensen J J, Kelkkanen A, Garcia-Lastra J M, Thygesen K S and Jacobsen K W 2010 *Phys. Rev. B* **81** 081408
[66] Wei M Z, Chen L, Lun N, Sun Y Y, Li D Y and Pan H Z 2011 *Solid State Commun.* **151** 1440